Design, Fabrication, and Alignment of the SuperCam Telescope Relay Optics

M. Borden[1], D. Golish[1,2], C. Drouet d'Aubigny[1,2], C. Groppi[3], J. Kloosterman[1], T. Cottam[1], X. Xu[1], D. Lesser[1], S. Silva[1], C. Kulesa[1], C. Walker[1,2], B. Cuerden[1]

[1]Steward Observatory, University of Arizona, Tucson, AZ 85721 USA
[2]TeraVision Inc., Tucson, AZ 85705 USA
[3]School of Earth and Space Exploration, Arizona State University, Tempe, AZ 85287 USA

***Abstract*— SuperCam is a 64 pixel, λ=870 μm, superheterodyne camera designed to work with the 10m diameter Heinrich Hertz Telescope on Mount Graham, Arizona. Large imaging arrays were not anticipated when the telescope was originally designed. As a result, complex relay optics are required to adequately re-image the telescope focus on the detector array. After a brief review of SuperCam's optical and environmental requirements, we present the approach selected, along with novel modeling methods used to validate the design. The optical tolerances which drove the opto-mechanical design are presented. New metrology and optical alignment methods developed for SuperCam, but equally applicable to other THz optical systems, are also discussed.**

I. INTRODUCTION

1.1 SuperCam Science and Instrument Design

SuperCam has been designed to operate in the astrophysically rich 870μm atmospheric window. The Heinrich Hertz Submillimeter Telescope has a 15μm RMS surface, making it one of the most accurate large submillimeter telescopes currently in operation. In addition, the 10,500ft elevation site on Mt. Graham offers weather sufficient for observing in this window more than 50% of the observing season, 24 hours per day. The receiver is an 8x8 array constructed from integrated 1x8 mixer modules, with state of the art mixer, local oscillator, low noise amplifier, cryogenic and digital signal processing technologies. In the past, all heterodyne focal plane arrays have been constructed using discrete mixers, arrayed in the focal plane. SuperCam reduces cryogenic and mechanical complexity by integrating multiple mixers and amplifiers into a single array module with a single set of DC and IF connectors. These modules are housed in a closed-cycle cryostat with a 1.5W capacity 4K cooler.

SuperCam has four times the number of pixels of any existing spectroscopic imaging array at submillimeter wavelengths. The exceptional mapping speed provided by 64 pixels, combined with the efficiency and angular resolution provided by the HHT will make SuperCam a uniquely powerful instrument for probing the history of star formation in our Galaxy and nearby galaxies. SuperCam will be used to answer fundamental questions about the physics and chemistry of molecular clouds in the Galaxy and their direct relation to star and planet formation. Through Galactic surveys, particularly in CO and its isotopomers, the impact of Galactic environment on these phenomena will be realized [1].

1.2 Environmental Constraints at the Telescope

The HHT was constructed before submillimeter array receivers became common. The instruments designed for the HHT typically reside at the Nasmyth foci to either side of the primary optical axis. The Nasmyth foci are located along the elevation axis of the telescope. A rotating tertiary in the apex room (which rotates with the telescope in elevation) allows instruments to be mounted on either side. However, the clear apertures of the elevation bearings on either side of the apex room are only 100 and 300 mm in diameter. Unfortunately, the size of SuperCam's beam footprint precludes putting the receiver past these narrow openings. The remaining option is to install the receiver in the apex room itself, which, among other challenges, limits the size of the system.

II. DESCRIPTION OF THE SUPERCAM OPTICAL DESIGN

The HHT's secondary provides Nasmyth instruments with an f/13.8 beam. The desired number of pixels for SuperCam requires a lower f/# if they are to fit in a reasonably-sized cryostat. One of the goals of our optics is to transform the incoming f/13.8 beams into f/5 beams that will couple efficiently with the receiver feedhorns.

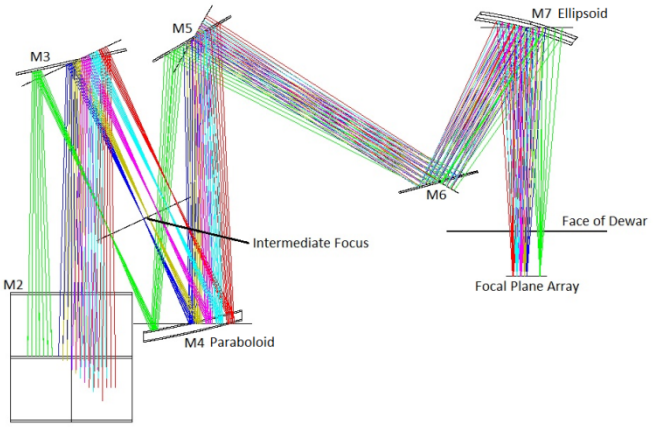

only the optics mounted on the wall are shown.

The SuperCam optical design, schematically pictured in Figure 1, is relatively simple. The system has two powered mirrors. The first is a parabolic mirror which essentially collimates the light from the telescope after it has come to a focus, the second is an elliptical mirror that focuses the beams to match the f/# of the feedhorns. Practical constraints force the system to include a number of flat mirrors, first to provide enough optical path for the telescope beam to come into focus, and then to provide the distance between the two powered mirrors which is required to provide adequate pixel separation and maintain image space telecentricity. The first flat mirror moves into the beam to direct it to the back wall of the apex room where the SuperCam optical support structure is mounted. The next two flat mirrors provide optical path length to let the beams come to focus before they reflect off the parabolic mirror. Two additional flats provide optical path between the parabolic and elliptical mirrors to set the beam spacing and image space telecentricity [1,2]. A CAD model of the receiver and its optics mounted in the apex room is shown in Figure 2.

III. OPTICAL TOLERANCES

For SuperCam to achieve adequate optical performance, an error budget was used to allocate error throughout the system. This budget includes the alignment tolerances of the SuperCam relay optics, the mirror fabrication errors, design residuals of the relay optics, errors associated with Optical Support Structure (OSS) deformation and errors in the alignment procedure, errors corresponding to FARO Arm measurement accuracy, and errors from the telescope. This error budget is shown below in Table 1.

Table 1: Error Budget for SuperCam Optical Tolerancing

Source of Error	**Resulting WFE**
Mirror Alignment	λ/33.6
Mirror Fabrication	λ/34.1
Design Residuals	λ/34.2
OSS Deflection / Alignment Procedure Errors	~0
FARO Arm Measurement Accuracy (Alignment)	λ/31
HHT Errors	λ/30
Total	λ/17.75

When added in quadrature the collective errors were λ/17.75, which met the allowable error requirement.

IV. TESTING OF OPTICAL COMPONENTS

4.1 Measurement and Data Processing

A portable CMM was used in this application. The FARO Quantum Arm, which has a measurement range of 8' in diameter, is an articulated metrology arm capable of measuring complex objects and assemblies in a single dataset to a volumetric accuracy better than 30 µm. It was used to measure the surface of each THz optic. The mirror was

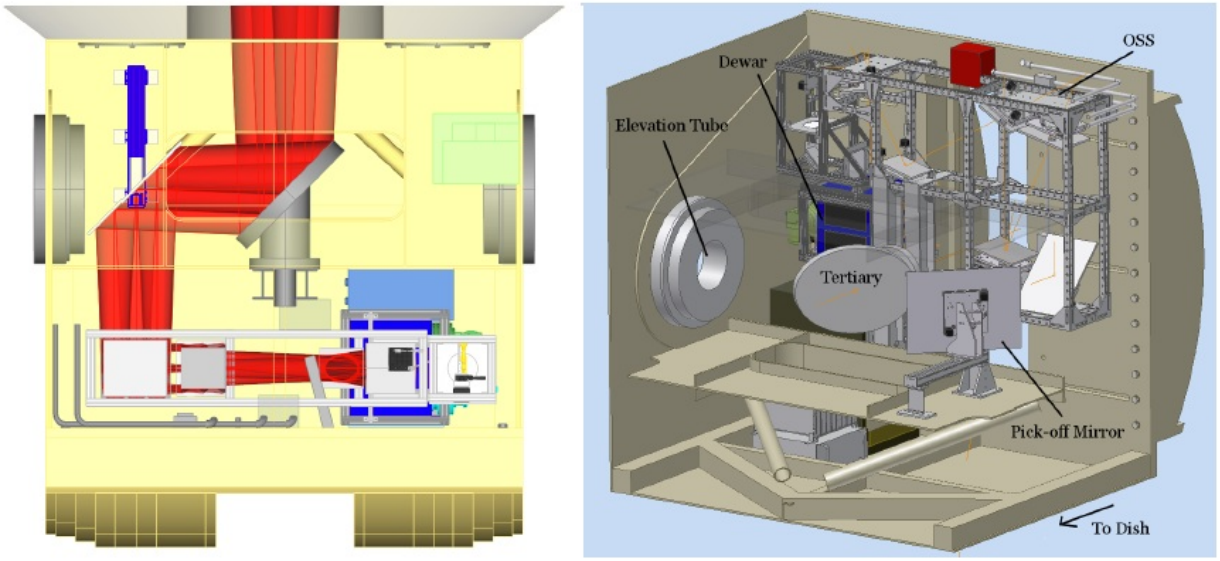

Figure 2: *CAD model of SuperCam and its optics mounted on the back wall of the SMT apex room. Left – Top view showing the beam bundles (in red) passing through the SMT primary mirror and into the apex room. Right – SuperCam relay optics seen within apex room. (Groppi 2009)*

mounted rigidly and data points were collected covering the entire surface of the optic.

As is common with CMMs, each measured coordinate is taken at the center of the spherical metrology probe. The result is a point which is offset by an amount equal to the radius of the probe along a vector normal to the surface. This was corrected using an algorithm in MATLAB. The resulting dataset represented the as-built optical surface. The theoretical surface was exported from Zemax. Using an optimizer in Spatial Analyzer® to best-fit the as-built optical surface to the theoretical optical surface, a dataset representing the difference between the two was generated. This difference dataset represented the fabrication errors associated with the as-built optical surface.

It was found that both mirrors were fabricated with an imperfect radii of curvature. The resulting fabrication error was found to be 26.5 μm rms for mirror M7 and 21.1 μm rms for mirror M4.

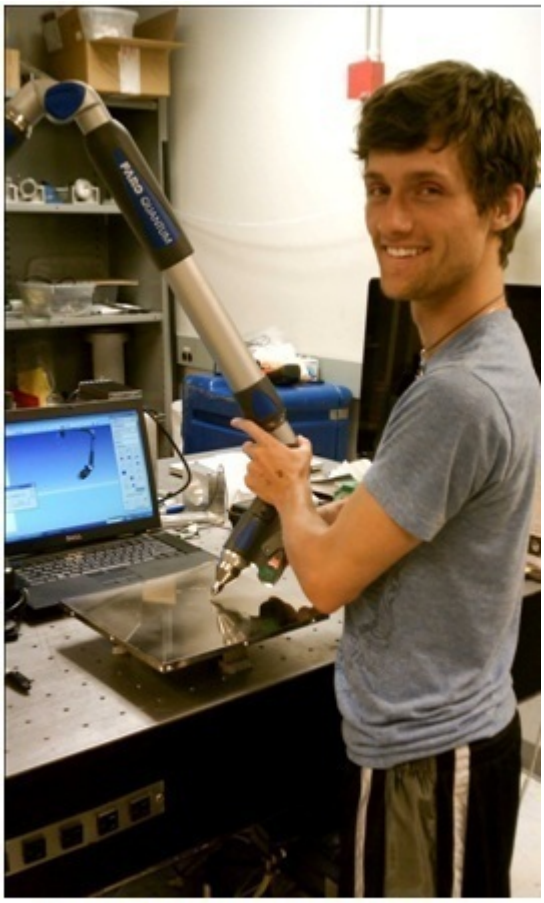

Figure 3: *Author using FARO Arm to measure optical surface of mirror*

4.2 Evaluation of effect of Mirror Fabrication Errors on Optical Performance

Zernike polynomials were used to represent the fabrication error dataset. These Zernike polynomials were incorporated into the original optical model in Zemax. We determined that these surface figure inaccuracies degraded the optical performance of the system from the design residuals of λ/34 to λ/32.25 in RMS wavefront error. Though the two powered mirrors were not fabricated perfectly, the resulting errors associated with their as-built surface figures were acceptable.

V. OPTICAL ALIGNMENT

5.1 Creating Reference Fiducials and Updating Mirror CAD Models

Using the FARO Arm as a tool for aligning THz optics has two major advantages: the surfaces of the optics do not need to be polished to optical quality and the loose tolerances allowed by THz optical systems is conducive to using an articulated metrology arm. A challenge of using an articulated metrology arm for alignment is that constraining the position of the measuring probe on the optical surface of each mirror is difficult making it an undesirable reference surface for alignment. To compensate for this, a set of mechanical reference fiducials were created to fully constrain the probe. This ensures repeatable measurements. These fiducials were machined into the sides of each mirror in the system and their positions in relation to the optical surface were measured. The position of these fiducials between mirrors thus became the new reference for mirror alignment.

The measured reference fiducials were then added to the CAD models of each mirror. This was done using the Spatial Analyzer® optimization which best-fits the as-built surface of the mirror to its theoretical surface. The as-built surface dataset included the measured fiducial positions. Thus the best-fit procedure coupled the positions of the fiducials to the theoretical surface of the mirror.

5.2 Using FARO Arm and Spatial Analyzer® for Mirror Alignment

The FARO Arm was then registered to the optical assembly by measuring the accessible fiducials of one mirror, which was considered the reference mirror of the system (in our case the elliptical mirror). Theoretical points were then created in Spatial Analyzer® corresponding to each of these measured fiducials. The measured fiducials were best fit to their theoretical positions using Spatial Analyzer®. The remaining mirrors in the system were then one by one, iteratively aligned to this first mirror. Three reference fiducials from each mirror were measured and compared to their theoretical position as determined by the CAD model. The difference between the two was minimized to an acceptable level by adjusting the position of the mirror. It should be noted that as each mirror is aligned, it is aligned with respect to the first mirror in the system, not the mirror next to it in the mirror assembly. This prevents alignment errors from accumulating between mirrors. We found this procedure provided an accurate and simple quantitative feedback mechanism for aligning THz mirrors.

VI. CONCLUSION

We found the FARO Arm to be an effective metrology tool for both verifying the surface of and aligning THz optics. Using the FARO Arm and the developed surface verifying

procedure, the surface figure of both powered mirrors was found to have imperfect radii of curvature. The resulting wavefront error at the pixel array as a result of these imperfect mirrors was λ/32.25.

Using the FARO Arm as an alignment instrument was very successful. The reach of our 8' Arm was adequate for aligning every mirror in the system to our reference mirror. The fiducials that were machined into each mirror provided a feature that was measured with consistency. Using these fiducials as alignment points, each mirror was referenced to the alignment mirror. This alignment process was iterative and was used until each reference fiducial being measured fell within adequate alignment tolerance for that mirror.

The remaining sources of error are the design residuals of the relay optics, the deflections of the Optical Support Structure and errors in the alignment procedure, errors corresponding to FARO Arm measurement accuracy, and the telescope figure and alignment errors. These errors together with the mirror fabrication errors and those associated with the alignment procedure account for a total error of λ/17.75.

REFERENCES

[1] Groppi, C., Walker, C., Kulesa, C., Golish, D., Kloosterman, J., Weinreb, S., Jones, G., Barden, J., Mani, H., Kuiper, T., Kooi, J., Lichtenberger, A., Cecil, T., Puetz, P., Narayanan, G., Hedden, A. "Testing and Integration of Supercam, a 64-Pixel Array Receiver for the 350 GHz Atmospheric Window." 2009. *SPIE*, Vol *7741*.

[2] Groppi, C., Walker, C., Kulesa, C., Golish, D., Kloosterman, J., Weinreb, S., Jones, G., Barden, J., Mani, H., Kuiper, T., Kooi, J., Lichtenberger, A. "Testing and Integration of Supercam, a 64-Pixel Array Receiver for the 350 GHz Atmospheric Window." 2010. *International Symposium on Space Terahertz Technology. 21st Annual ISSTT Proceedings.* 23-25